

# Low voltage fault ride-through operation of a photo-voltaic system connected utility grid by using dynamic voltage support scheme

Satyanarayana Burada<sup>1</sup>, Kottala Padma<sup>2</sup>

<sup>1</sup>Department of Electrical and Electronics Engineering, Anil Neerukonda Institute of Technology & Sciences (ANITS), Visakhapatnam, India

<sup>2</sup>Department of Electrical Engineering, Andhra University, Visakhapatnam, India

## Article Info

### Article history:

Received Dec 16, 2024

Revised May 31, 2025

Accepted Jul 23, 2025

### Keywords:

Active current

Dynamic voltage support system

Energy storage unit

Grid network

Low voltage ride through

Reactive current

Trip

## ABSTRACT

This research suggests a control technique that makes use of a microgrid's energy storage and to enable low voltage ride through (LVRT) process with a flexible dynamic voltage support (DVS) system. First, the requirements for the microgrid's maximum DVS are stated, together with an explanation of how these requirements depend on the characteristics of the analogous network that the microgrid sees. In order to create a flexible DVS regardless of the changing system circumstances, reference signals for currents that are derived from maximum voltage tracking technique are suggested in this research. These signals take into account the challenges involved with real time parameter assessment in the context of transient voltage disruptions. Second, a control scheme is suggested to allow a microgrid's energy storage-based LVRT operation. Thirdly, a novel approach to energy storage sizing for LVRT operation is offered, taking into account the corresponding network characteristics, grid code requirements, and the rated current value of the power electronic converter. Real-time MATLAB simulations for low-voltage symmetrical faults are used to validate the suggested control technique.

*This is an open access article under the [CC BY-SA](https://creativecommons.org/licenses/by-sa/4.0/) license.*



## Corresponding Author:

Satyanarayana Burada

Department of Electrical and Electronics Engineering

Anil Neerukonda Institute of Technology & Sciences (ANITS)

Visakhapatnam, Andhra Pradesh 531162, India

Email: satyanarayana.eee@anits.edu.in

## 1. INTRODUCTION

In light of their growing penetration, the requirement for mandated services such as voltage fault ride-through (VFRT) functioning from microgrid/photovoltaic unit (PV unit) is increasingly essential to preserving the utility grid's reliability and permanence. According to the grid code [1], the VFRT technique necessitates that the grid-connected photovoltaic unit remain linked to the microgrid until the voltage differences maintain within a VFRT characteristic curve. The generator unit is also responsible for maintaining the nearby voltage by regulating the active and reactive power of its total power production. In addition to requiring VFRT operation from the DER, the IEEE 1547:2018 norm, which was just released, also included a number of other features, such as multiple performance areas that come under the VFRT characteristics, needs for dynamic voltage support (DVS), microgrid unusual performance group classification, and consecutive VFRT needs [2]. The potential of the grid-following PV unit with inverter-connected DVS to swap an appropriate amount of current with the network during extreme voltage fluctuations enhances the network's voltage profile and averts situations that can cause VFRT or trip operations. The main variables that dictate how much voltage support

the grid-following PV unit can provide are its current output's magnitude and phase angle [3]. For the purpose of maintaining voltage within limits during the VFRT operation, a variety of centralized and decentralized techniques that depend on the current control of the power electronic converter are outlined in the works. This addresses control that relies on a steady reactive current [4], voltage variation with reactive current [5], [6]. The authors in [7] use a reactive power modulator approach to assist and improve the voltage by computing the standard or reference value for reactive power. This approach takes into consideration both the reactive power produced by the positive sequence voltage at the point of common coupling (PCC) and the capacitor used in the filter. When necessary, the aforementioned techniques reduce real power in order to make space to provide the continuous reactive power needed in the event of severe voltage swings. The utility grid's medium and high voltage portion, when the ratio of the lines' reactance to resistance ( $X/R$ ) is large, is the only area where DVS operation has proven effective, despite encouraging findings. Reactive current dependency on voltage support is shifted to real current injection through distribution feeders of the microgrid with low values of  $X/R$ . A few pieces of literature discuss the DVS from the PV unit that is integrated to the grid with facing low voltage profile. A sensitivity evaluation is performed [8], and the maximum current limit of the inverter [9] is used to optimize real current infusion over the voltage sag as the basis for current control. This improved the voltage; However, it is not to the maximum or peak voltage that is necessary for VFRT operation under substantial fluctuations in voltage. Furthermore, not one of the aforementioned techniques can provide the DVS while adapting to changing network conditions.

The study by Camacho *et al.* [3] shows how the inverter's maximum voltage support depends on the network's  $X/R$  ratio. If a mostly accurate real-time assessment of the fluctuating impedance of the grid is established, can the highest DVS be realized. An ideal voltage support control for low-voltage grids experiencing faults is suggested in [10]. To make the DVS operational while performing the VFRT procedure, the authors, however, made the assumption that the grid's  $X/R$  ratio was known in advance and proposed that wide-band system identification techniques be used to get the grid's  $X/R$  ratio [11], [12]. Nevertheless, a number of variables, such as the perturbation signal's magnitude and bandwidth and the existence of dynamic components within the system, affect how accurate these approaches are. After conducting a thorough quantitative examination, the writers have ascertained that a couple of additional characteristics of the comparable network seen by the PV unit, which the following section addresses, as well as the reactance to resistance ratio of the Thevenin impedance across the microgrid network, determine the peak voltage that the PV unit can support. The electric grid's dynamic nature and the fault voltage's brief duration make it extremely difficult to measure or estimate near-accurate equivalent network metrics in real-time. In order to provide maximal DVS despite fluctuating network conditions, there is an immediate requirement to generate inverter current comparisons despite genuinely analyzing similar system characteristics. It may occasionally be necessary to constrain real current during voltage support during VFRT operation in order to allow space for reactive current, provided that the PV system functions at the maximum power point tracking (MPPT) state [13]. This would result at the inverter's DC link, there is a disparity. using an electrical energy storage device at the DC bus or a crowbar network [14], [15], using off-MPPT state for the PV source, and oversizing the inverters [16] are a few potential options. The cost of energy storage technologies has decreased, and their application areas have expanded due to recent advancements in the field [17]. The technique, which is connected with an energy storage device used at the inverter's DC bus, stores solar power that would otherwise be wasted and can offer extra functions to the utility grid or microgrid, such as electrical inertia, black start operation, fast frequency reserves, and frequency fault ride-through assistance. Additionally, the network voltage can be supported by the energy storage during periods of low generating outputs from solar PV units [18]. There is currently no general approach that measures the energy storage's contribution to fault ride-through operation and its sizing design for this approach. Furthermore, in light of fault ride-through performance using energy storage devices, managing the storage of electrical energy in concert with additional renewable energy sources and storing elements essential to achieving adaptive DVS-based VFRT operation [19].

The discussion above makes it clear that a control strategy that ensures a DVS that is responsive to shifting networking circumstances amid significant voltage fluctuations and permits VFRT microgrid performance in fluctuating system conditions, while taking into account perhaps the involvement of the microgrid's built-in power reserve, has not yet been acknowledged. Below is the summary of the work's principal accomplishments.

- Utilizing the extreme voltage tracking (EVT) method, a flexible DVS approach determines the microgrid output characteristics of active current to enable optimal voltage support at the interconnected point of grid and inverter, called as point of common coupling (PCC), and produces reference values for active and reactive current in the event of an external voltage defect.
- Flexible DVS with baseline parameters for currents, fault detection, and energy storage control are all combined in this control method to enable low-voltage fault ride-through functioning of the system.
- A novel approach to assessing the role of a microgrid's energy storage based on the inverter maximum current rating, the VFRT characteristic, and potential adverse comparable network configurations to assess

whether there is enough storage capacity of electric energy to support the fault ride-through operation with the suggested DVS approach.

## 2. VOLTAGE CONTROL AND REACTIVE POWER MANAGEMENT BY MICROGRID

Figure 1 [4] shows an identical network of the system. The PV unit and inverter represent a current resource ( $\vec{I}_{inv,pu}$ ), the filter impedance and impedance of the local load are modelled with  $Z_{filt,pu}$ , the line impedance that joins the substation with the microgrid is designed as  $Z_{ln,pu}$ , the remaining load impedance at the substation is taken as  $Z_{ex,pu}$ , the fault impedance is given as  $Z_{F,pu}$ , at the substation, and it is  $Z_{m,pu}$  beyond it and  $V_{m,pu}$ . The following expression provides the corresponding Thevenin impedance observed across the inverter points at the time of fault conditions.

$$|Z_{th,pu}| \angle \zeta = R_{th,pu} + jX_{th,pu} = \frac{Z_{filt,pu}Z_{ln,pu} + Z_{filt,pu}Z_{X,pu}}{Z_{filt,pu} + Z_{ln,pu} + Z_{X,pu}} \quad (1)$$

Where (2):

$$Z_{X,pu} = \frac{Z_{ex,pu}Z_{F,pu}Z_{m,pu}}{Z_{ex,pu}Z_{F,pu} + Z_{ex,pu}Z_{m,pu} + Z_{F,pu}Z_{m,pu}} \quad (2)$$

in a similar vein, the microgrid's Thevenin voltage is listed as (3).

$$|V_{th,pu}| \angle \delta = \frac{Z_{filt,pu}^2 Z_{Y,pu} + Z_{filt,pu} Z_{ln,pu} Z_{Y,pu}}{(Z_{Y,pu} + Z_{m,pu})(Z_{filt,pu}^2 + Z_{ln,pu}^2) + \alpha} \times V_{g,pu} \quad (3)$$

In (4) and (5).

$$Z_{Y,pu} = \frac{Z_{ex,pu}Z_{F,pu}}{Z_{ex,pu} + Z_{F,pu}} \quad (4)$$

$$\alpha = 2Z_{filt,pu}(Z_{ln,pu}Z_{m,pu} + Z_{ln,pu}Z_{Y,pu}) + Z_{filt,pu}Z_{m,pu}Z_{Y,pu} + Z_{ln,pu}Z_{m,pu}Z_{Y,pu} \quad (5)$$

Figure 2 depicts a modified comparable circuit with a balanced fault, taking into account  $|V_{th,pu}| \angle \delta$  and  $|Z_{th,pu}| \angle \zeta$ . As a result, the inverter voltage is expressed as (6).

$$V_{inverter,pu} = |V_{th,pu}| \angle \delta + |I_{inv,pu} \times Z_{th,pu}| \angle (\beta + \zeta) \quad (6)$$

Where  $\beta$  is the angle made by the inverter current with the voltage and  $|V_{th,pu}| \angle \delta$  is the Thevenin equivalent voltage noticed at the common coupling point when the microgrid is not providing any current, and the subsequent term is the support voltage that came about as a result of the microgrid's current provision. The (7) is a display of the PCC voltage indicated in (6).

$$|V_{inv,pu}| = \sqrt{V_{th,pu}^2 + \Delta V^2 + 2|V_{th,pu} \times \Delta V| \cos(\delta - \beta - \zeta)} \quad (7)$$

Where (8):

$$\Delta V = I_{inv,pu} \times Z_{th,pu} \quad (8)$$

here  $\beta$  stated positive sequence current components of the microgrid's current.

$$\beta = \tan^{-1} \left( \frac{i_{inv,pu}^{(q)}}{i_{inv,pu}^{(d)}} \right) \quad (8)$$

Where  $i_{inv,pu}^{(d)}$ ,  $i_{inv,pu}^{(q)}$  represents the respective positive sequence components of active and reactive currents of the microgrid. Using (7) and (8), the relationship that ensues is created to attain higher voltage scenarios.

$$\left( \frac{i_{inv,pu}^{(q)}}{i_{inv,pu}^{(d)}} \right) = \tan(\delta - \zeta) \quad (9)$$

It is recommended to operate the microgrid as an active power sink at lower field excitation cases and an active source of energy at higher excitation cases, respectively, to achieve the higher and lower values of voltage at the common coupling point according to (9). This indicates that the reference values of active and reactive current should be negative and positive for the under-excitation cases, and the other way around for the over-excitation scenario of the microgrid. The current produced by the microgrid at excessive voltage at the common coupling point is solely determined by  $\zeta = \tan^{-1} \left( \frac{X_{th,pu}}{R_{th,pu}} \right)$  which is called as impedance angle when  $\delta \approx 0$  (because of PLL synchronization or network conditions). But usually  $\tan(\delta - \zeta)$  is used to generate current references instead of  $\tan \zeta$ , when  $\delta \neq 0$  (during transients). With reference to (6), the maximum and lowest voltage magnitudes are dependent on the values of  $|V_{th,pu}|$ ,  $|I_{inv,pu}|$  and  $|Z_{th,pu}|$ . They remain constant despite variations in  $\delta$  and  $\zeta$ , provided that  $|Z_{th,pu}|$  remains constant. The maximum DVS is facilitated by altering the reference values for the active and reactive currents ( $i_{inv,pu}^{(d)*}$ ,  $i_{inv,pu}^{(q)*}$ ) of the inverter in accordance with (9), depending on the optimum current capability of the inverter  $|I_{inv,pu}^{max}|$  listed below. This is because the ratio of the direct and quadrature components of current in the inverter ( $i_{inv,pu}^{(d)}$ ,  $i_{inv,pu}^{(q)}$ ) when the highest voltage is achieved is relied on  $\delta$  or  $\zeta$ , or two of them, as shown in (9).

$$\sqrt{(i_{inv,pu}^{(d)})^2 + (i_{inv,pu}^{(q)})^2} = |I_{inv,pu}^{max}| \quad (10)$$

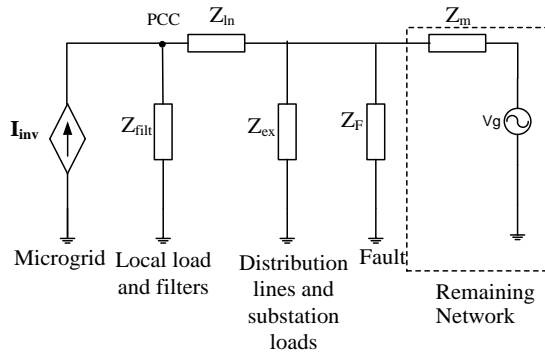


Figure 1. An identical network of a microgrid interfaced to the grid

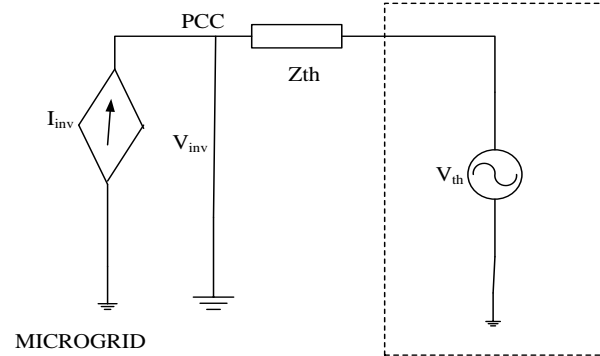


Figure 2. Modified comparable circuit with balanced fault

### 3. CONTROL DESIGN FOR LVRT TECHNIQUE OF A MICROGRID

Figure 3 presents an analyzed system for grid grid-interfaced microgrid and a suggested controlling approach. It expands the analogous circuit of Figure 1. A grid-connected inverter connects the PV unit and energy storage device, which make up the microgrid, to the remaining network at the point of common coupling via their respective converters [4]. This graphic shows the control scheme used to allow VFRT functioning of a microgrid with an adaptive dynamic voltage support scheme. The control strategy primarily covers the grid-connected inverter, energy storage converter, and PV unit converter controllers.

#### 3.1. PV unit controller

The MPPT algorithm is used to regulate the unidirectional converter (DC-DC) connecting a PV unit, allowing it to draw the maximum power out of the PV unit even when the VFRT function is in progress. To do this, the MPPT controller receives measured data from the PV terminal voltage and current ( $v_{pv}$ ,  $i_{pv}$ ) which it uses to create the switching pulses to the unidirectional DC-DC converter through the duty cycle ( $D_{pv}$ ).

#### 3.2. Controller for storage of electrical energy

Predicated on the DC bus signaling methodology, a control mechanism scheme [20] is developed to regulate the input voltage for the inverter and enable the power control between different gadgets that communicate with the DC line. The energy storage only activates as soon as the voltage at the DC line changes from the nominal voltage ( $v_{dc,pu}^*$ ) by more than  $\pm 2.5\%$  and regulates it within  $\pm 5\%$ . In contrast, the inverter regulates the voltage at the DC link until  $\pm 2.5\%$  of 1 pu. With reference to Figure 3, the voltage deviation associated with the DC bus voltage ( $v_{dc}$ ) is computed once it is calculated and transformed into the per unit

value ( $v_{dc,pu}$ ). The dead-zone block guarantees the deviation in voltage that is greater than  $\pm 2.5\%$  of  $v_{dc,pu}^*$  are only sent to the controller or regulator, which uses the PI controller to generate  $i_{ess,pu}^*$  which is reference value of the current in the energy storage device. The current controlling technique ensures that the energy storage unit observed per unit current ( $i_{ess,pu}$ ), complies with the supplied baseline and produces the appropriate duty cycle ( $D_{ess}$ ), which generates pulse width modulation pulses. The DC crowbar technology dissipates surplus power into heat energy, restricting the DC link voltage at  $+5\%$  [21].

### 3.3. Grid-connected inverter controller

According to Figure 3, the inverter connected to the DC link operates during VFRT operation by obtaining triggering pulses through a pulse width modulation approach according to the recommended reference values for active and reactive current. The voltage and current values of the filter ( $v_{inv}, i_{inv}$ ), which are the local variables, are transformed into values per unit and supplied to the controller. Using the Park transformation, an enhanced phase-locked loop (PLL) determines the data regarding  $\gamma$  which is the phase angle of  $v_{inv}$  and uses it to compute the current and voltage component values in the form of dq-axis ( $v_{inv,pu}^{(dq)}, i_{inv,pu}^{(dq)}$ ) [22]. In addition,  $v_{inv,pu}$  is compared to the IEEE 1547:2018 standards' APC-II VFRT characteristic in order to identify the VFRT state and to activate or deactivate the TRIP signal, as well as a string of VFRT events [2]. While the active current reference ( $i_{inv,pu}^{(d)*}$ ) of the inverter is obtained during stable operation of the system, the reference value for reactive current ( $i_{inv,pu}^{(q)*}$ ) can be produced through appropriate PI controllers. The current controller device, flexible dynamic voltage support approach takes the use of voltages along with inverter currents in dq axis form ( $v_{inv,pu}^{(dq)}, i_{inv,pu}^{(dq)}$ ) to produce  $\frac{i_{est,pu}^{(q)}}{i_{est,pu}^{(d)}}$  and to monitor the reference values of current signals [23].

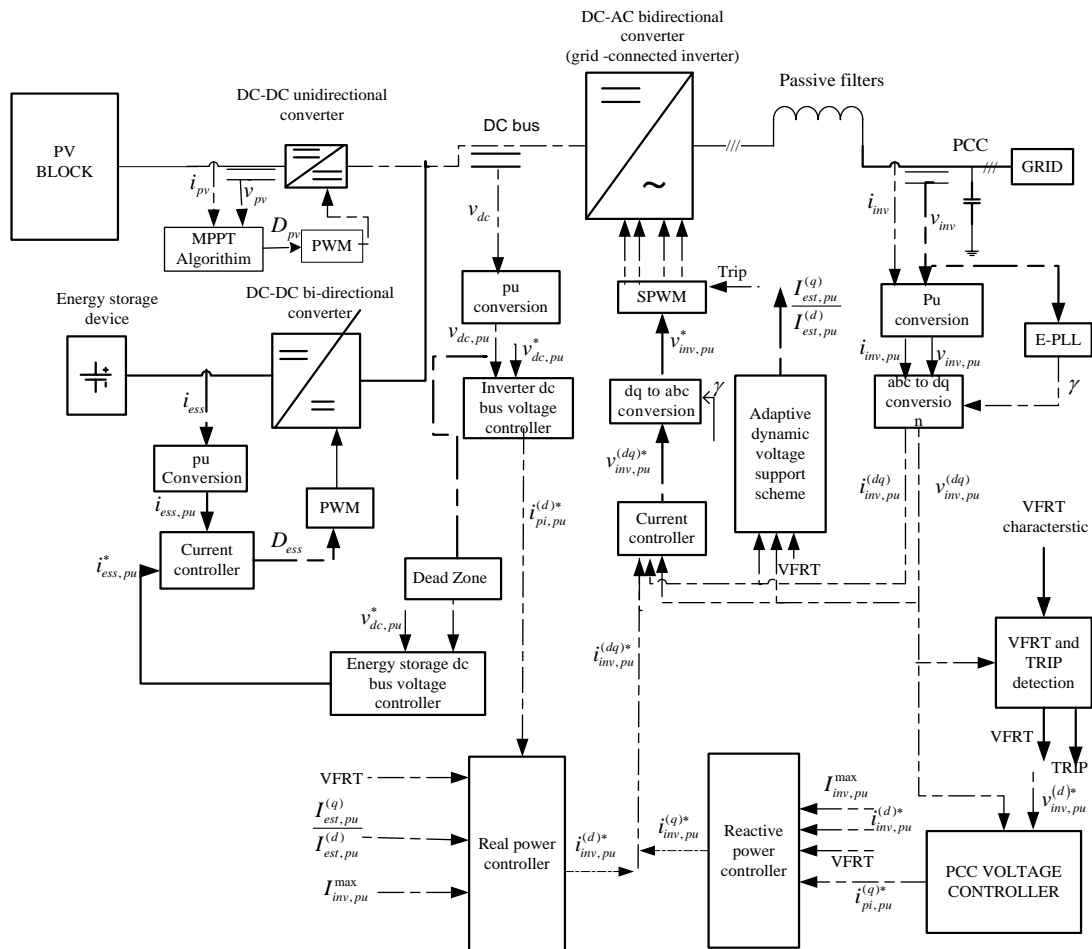


Figure 3. Suggested a controller to regulate the VFRT functioning of the system

The real and reactive power controllers, respectively, create the inverter's suitable reference values for the currents ( $i_{inv,pu}^{(d)*}, i_{inv,pu}^{(q)*}$ ) depend on the suggested flexible DVS approach, when fault ride through is occurring circumstances on the network (VFRT = 1). The VFRT detecting block generates the Trip = 0 instruction and interrupts the SPWM pulses to the inverter in the situation when the voltage change is greater than the standard deviation of VFRT [24]. A DC bus and an efficient energy storage mechanism attached to the microgrid are needed for the suggested control approach using the adaptive DVS scheme. Consequently, the following section examines the function of the mechanism to store the energy and the ability needed for attaining the intended fault ride-through operation.

#### 4. FUNCTION AND DESIGN OF ENERGY STORAGE DEVICE

To make the suggested DVS scheme possible, energy storage must play a crucial role in preserving the microgrid's DC bus voltage. As a result, the storage device parameters like maximum energy and maximum power are determined with a flexible dynamic voltage approach to activate the fault ride through process for the system, and the amount of storage of electrical energy that is available is then assessed. Energy sent to the grid while maintaining a constant power supply is frequently impacted by variations in the PCC voltage. A disparity in power occurs at the DC link when the microgrid employs the PV unit's full output power. This imbalance results from the PV unit's maximum power output being less than the power supplied using the inverter. The following formula provides active power that is fed into the inverter.

$$P_{inv,pu} = v_{inv,pu}^{(d)} \times i_{inv,pu}^{(d)} \leq P_{pv,pu} \quad (11)$$

Where  $P_{pv,pu}$  is the DG unit's available power output. Nonetheless, active and reactive currents must be managed in order to supply flexible DVS, over VFRT performance according to network state within the inverter current capacity, according to the study conducted in section 2. In order to achieve the DVS while ensuring the inverter operates safely, the value of d-axis current to q-axis current ratio pumped from the inverter must therefore follow (9), and the inverter can supply peak current that is specified in (10). The power imbalance ( $P_{imb,pu}$ ) that occurs at the microgrid's DC bus during voltage changes is provided below using the expression for  $i_{inv,pu}^{(d)}$  from (11), where represents ( $P_{pv,pu} - P_{inv,pu}$ ) low voltage conditions and ( $P_{pv,pu} + P_{inv,pu}$ ) represents high voltage conditions.

$$P_{imb,pu} = P_{pv,pu} \mp P_{inv,pu} = P_{pv,pu} \mp \frac{v_{inv,pu}^{(d)} \times I_{inv,pu}^{max}}{\sqrt{1 + \left( \frac{I_{est,pu}^{(q)}}{I_{est,pu}^{(d)}} \right)^2}} \quad (12)$$

To keep the DC bus voltage steady, energy storage must be used to reduce this brief but noticeable power disparity at the DC link. For low voltage fault conditions,  $v_{inv,pu}^{(d)}$  is maintained at 1pu, with  $I_{inv,pu}^{max} = 1.2$  pu being the default value. The minimal and maximum generation from the PV unit are represented by the contours for  $P_{pv,pu} = 0$  pu and 1 pu, respectively [25]. The energy storage device must charge in order for  $P_{imb,pu}$  to be positive, and vice versa. Therefore,  $P_{imb,pu}$  can be used to determine the energy storage device's maximum power rating. When  $v_{inv,pu}^{(d)}$  is replaced in (12) with the VFRT characteristic voltage, let  $P_{imb,pu}^{VFRT}$  represent the power disparity at the DC link or DC bus. the energy storage device's necessary power rating is provided by (13).

$$P_{storage,pu} = s \times \max(|P_{imb,pu}^{VFRT}|) \quad (13)$$

Where the safety factor ( $s=1.05$ ) takes into account the impact of the losses incurred during the power conversion phases. The electrical energy swapped by the storage device is also provided by (13), encompassing the impact of the quantity of VFRT occurrences ( $N_{VFRT}$ ). This is expressed in Watt-sec.

$$E_{storage} = N_{VFRT} \times \int_0^{t_{VFRT}} P_{storage,pu} \times P_b \times dt \quad (14)$$

Here  $t_{VFRT}$  is the VFRT characteristic's time in seconds, and  $P_b$  is the base power to transfer normal values into per unit. The necessary energy storage device's power and energy ratings are found using (13) and (14). This analysis can be used as a guide to confirm that the microgrid's current energy storage device is adequate

and, if necessary, to update it to incorporate the appropriate energy storage so that the flexible DVS methodology can support VFRT functioning.

## 5. SIMULATION RESULTS

A microgrid that stores energy using supercapacitors (SC) and photovoltaic solar power (PV) as distributed generators (DG), depicted in Figure 3, is examined using MATLAB software to simulate the suggested control strategy's performance. Table 1 contains a list of the system parameters. The basic values taken into account for each unit conversion are 50 Hz for frequency, 415 V for AC voltage, and 10 kVA for AC power and 10 kW for DC power. Since symmetrical faults typically have the worst possible impact within the system, in contrast to different kinds of failures, only symmetrical faults are taken into account in this simulation study. It is assumed that the inverter has a maximum current rating of 1.2 pu. A positive active power value is interpreted as it is delivered to the DC link or DC bus throughout this section, and conversely. Comparably, reactive power that is positive indicates that reactive power is being added to the grid. This study takes into account the maximum PV unit generation at every stage.

### 5.1. Low voltage fault ride-through operation for fault voltage within VFRT characteristics

The low-voltage ride-through (LVRT) operation of the microgrid is presented in this chapter. Figure 4 shows the irradiation curve during the course of 20 seconds. Figure 5 illustrates how the MPPT controller tracks the MPP with 99 percent efficiency. The system experiences a 3- $\phi$  fault at 3.5 sec for time of 2 s, creating a voltage of 0.671 per unit at the point of common coupling (PCC). Therefore, the VFRT pulse is activated during the fault time, and the VFRT detecting block generates the TRIP=1 instruction and continues the SPWM pulses to the inverter if there is a voltage disruption within the VFRT characteristics (as shown in Figures 6(a)-6(c)).

When a low voltage fault occurs, the inverter uses its 1.2 pu over-current limit and begins injecting actual and reactive current based on as shown in Figure 7. Accordingly, as seen in Figure 8, the inverter's active and reactive power is delivered into the system. Furthermore, Figure 9 shows the actual power exchanged between the energy storage device, the inverter, and the PV unit. To keep the voltage at the DC link or DC bus around  $\pm 1.05$  pu, the energy storage system's electrical power supply is modified based on the change in real power of the inverter. As the point of common coupling (PCC) voltage does not become less than the LVRT voltage during the fault time, the inverter remains connected to the grid, supplies reactive power (see Figure 10), and provides a dependable with steady fault ride-through functioning with no effect on the PV array's MPPT performance. With the suggested control technique, the voltage at the common coupling point is increased to 0.92 pu and the inverter supplies reactive power till the PCC voltage reaches its nominal value. (refer to Figures 11 and 12).

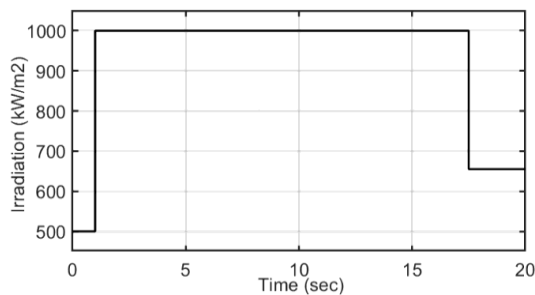


Figure 4. Irradiation curve

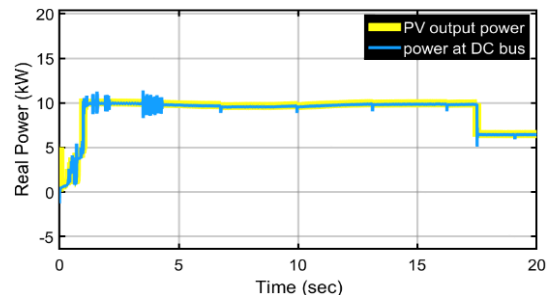


Figure 5. MPPT efficiency

Table 1. System specifications

Parameter	Value
PV Unit	15 modules of 37.3 V (voltage at MPP), 8.66 A (current at MPP); 10 kW (power at MPP)
Supercapacitor bank	20 units of 130 F, 50 V modules
DC-DC unidirectional converter	10 kW, 415/415 V, 10 kHz
Inverter connected to the grid	3 phase, 415(DC)/415 V(AC), 10 kVA, 10 kHz
Filters	450 VAR, 3 ph, C filter, L filter L = 6 mH
Three-phase transformers	220/415 V, 10 kVA, winding1 connection (Yg), winding2 connection (Delta (D1))
Rest of the network	3 phase, 415 V, 50 Hz, short circuit ratio = 8, X/R ratio = 0.5

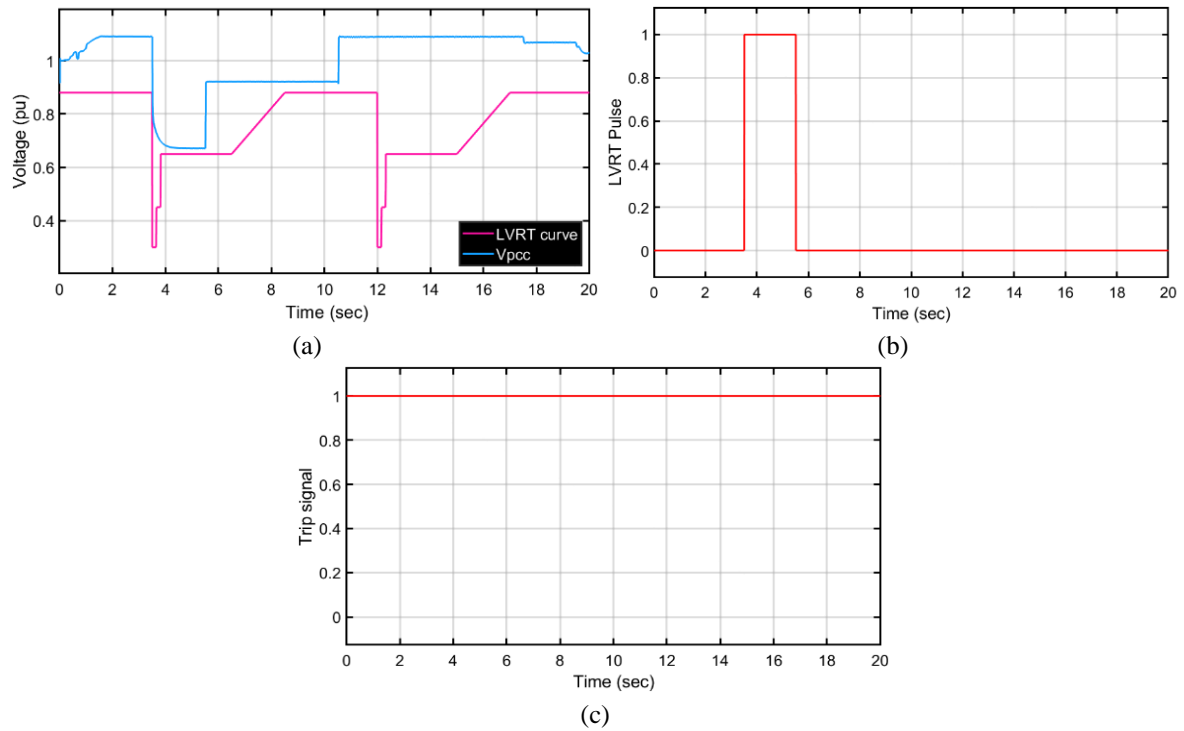


Figure 6. Fault ride-through parameters: (a) LVRT & PCC voltage, (b) LVRT pulse, and (c) TRIP signal

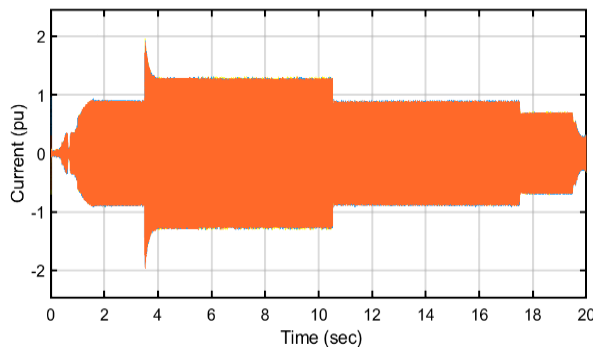


Figure 7. Inverter line currents

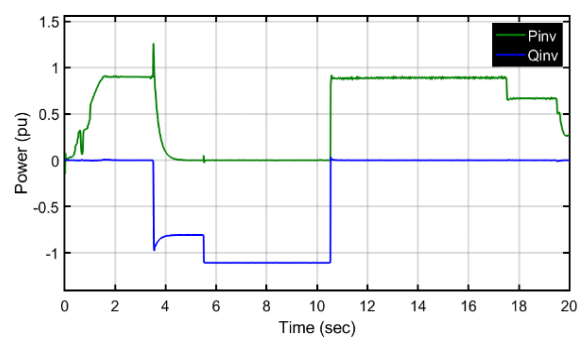


Figure 8. Inverter active and reactive power

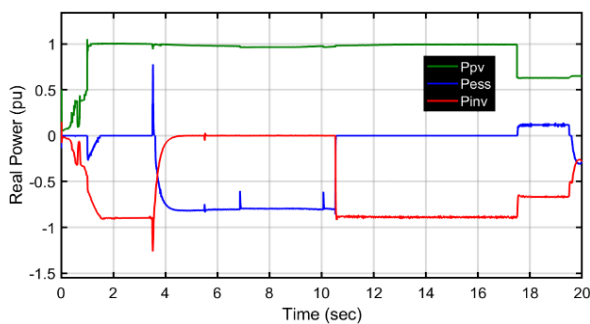


Figure 9. Real power of microgrid components

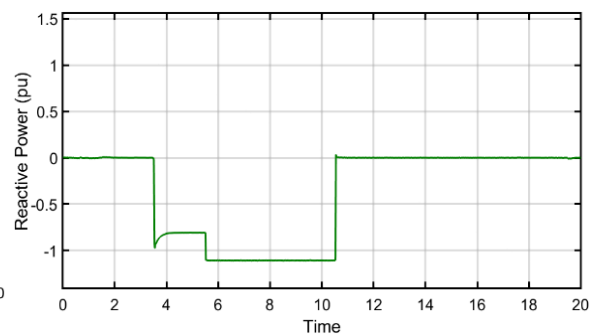


Figure 10. Reactive power from the inverter

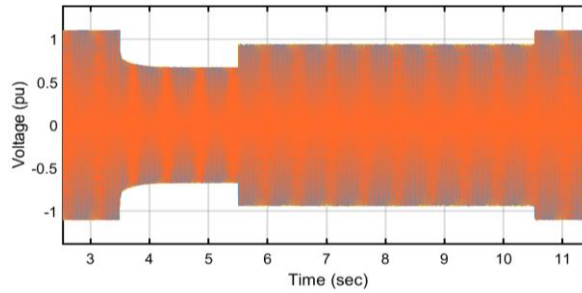


Figure 11. PCC phase voltages

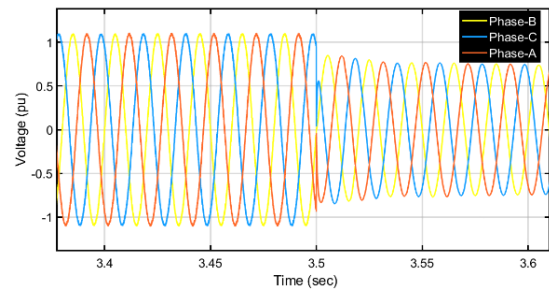


Figure 12. PCC phase voltages in a magnified view

## 5.2. Low VFRT operation for fault voltage exceeds VFRT characteristics

The LVRT process of the microgrid, if the voltage value at PCC exceeds the VFRT characteristics, is presented in this chapter. The system experiences a 3- $\phi$  fault with low fault impedance at 3.5 sec for a time of 2 s, creating a voltage at PCC less than VFRT characteristics as shown in Figure 13. In Figure 13, it is observed that the PCC voltage at 3.8 sec is 0.49 pu, which is less than the VFRT characteristics.

Therefore, the VFRT pulse is activated during the fault time, and the VFRT detecting block generates the TRIP = 0 instruction and interrupts the SPWM pulses to the inverter if there is a voltage disruption that exceeds the VFRT characteristics (refer to Figures 14(a) and 14(b)). When the VFRT detecting block generates the TRIP = 0 instruction and interrupts the SPWM pulses to the inverter, there is no connection between the inverter and the grid. Therefore, the inverter cannot transfer currents to the grid as shown in Figure 15.

Furthermore, Figure 16 shows the actual power exchanged between the energy storage device, the inverter, and the PV unit. When the grid is disconnected from the inverter, the PV power is transferred to the storage device. To keep the voltage at the DC link or DC bus around  $\pm 1.05$  pu, the energy storage system's electrical power supply is modified based on the change in real power of the inverter.

Furthermore, as seen in Figure 17, the inverter's active and reactive power is delivered into the system. It is observed in Figure 17 that the inverter supplies reactive power from fault occurrence time (3.5 sec) to 3.8 sec, when the inverter disconnects from the grid network there is no power transfer takes place from the inverter to the grid network. As the inverter is disconnected from the utility grid at 3.8 sec, after the fault clearance, the voltage at PCC will be equal to the grid nominal voltage, that is 1 pu as depicted in Figure 18. The PCC phase voltages in the zoomed version are shown in Figure 19.

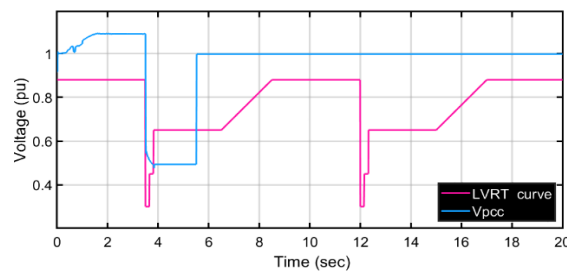
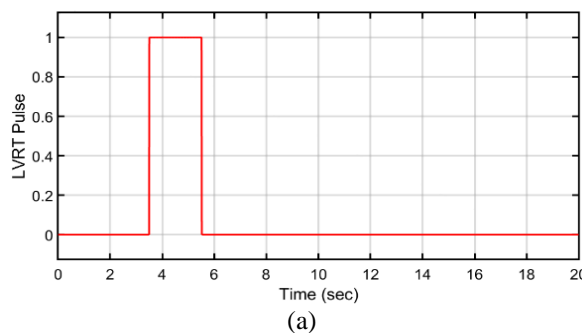
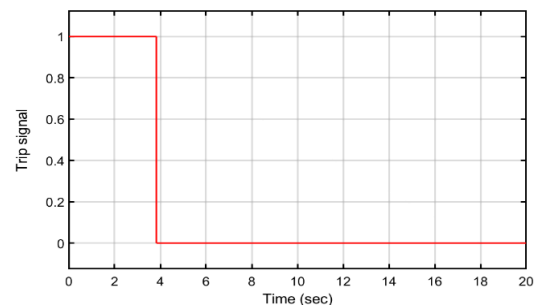


Figure 13. LVRT and PCC voltages



(a)



(b)

Figure 14. Fault ride-through parameters: (a) LVRT pulse and (b) TRIP signal

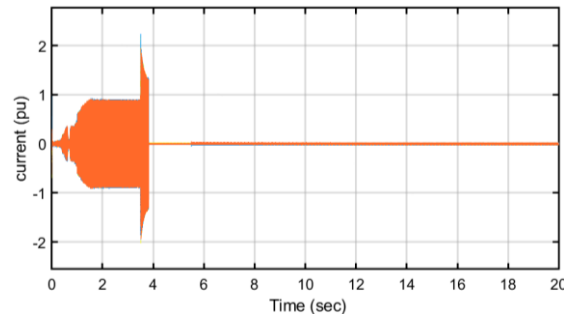


Figure 15. Inverter line currents

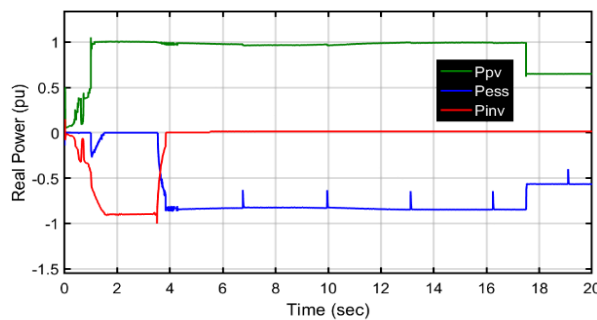


Figure 16. Real power of microgrid components

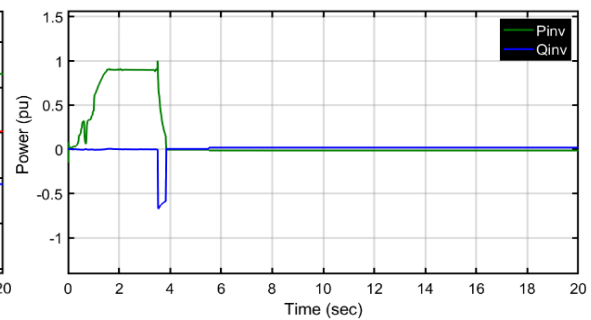


Figure 17. Inverter active and reactive power

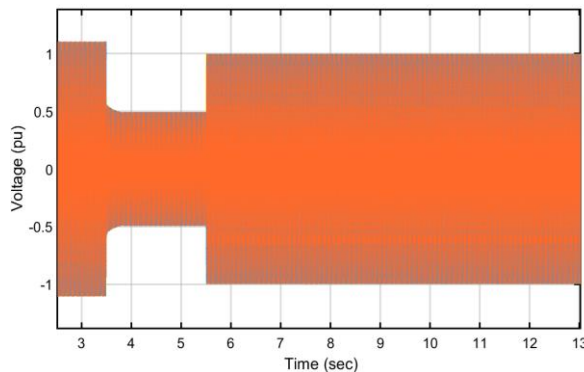


Figure 18. PCC phase voltages

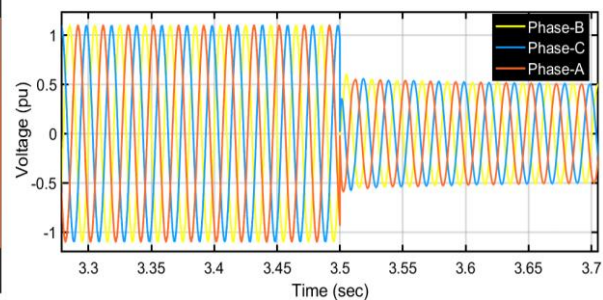


Figure 19. PCC phase voltages in a magnified view

## 6. CONCLUSION

The literature that is now accessible addresses VFRT problems; however, its approaches do not take into account the varying network situations present amid system malfunctions. Instead, they are solely on real, purely on reactive current, or a mix of the two. In this work, a control approach that makes use of the energy storage system's assistance is provided, and its effectiveness is assessed for a range of operating scenarios, including Several issues related to various fault voltages and low VFRT. In order to ensure the best DVS possible, the proposed DVS technique adaptively determines the microgrid's actual and reactive current output according to various circumstances developing throughout the VFRT procedure. With the suggested control strategy, it has been shown that a microgrid running at minimal VFRT values is capable of supplying flexible voltage assistance for unanticipated fault incidents within the grid, guaranteeing the inverter's secure functioning by abiding by the maximum current limit, and improving the utility grid's VFRT capability by tolerating more severe faults. This work's sizing technique for the storage device's necessary power rating serves as a guide for adapting the energy storage that is presently accessible towards modest VFRT running on a microgrid. Future research might examine how the microgrid functions in unbalanced fault scenarios, and suggest a strategy for managing the flexible DVS that makes use of both components of voltage and current in the positive and negative sequence throughout VFRT functioning.

## FUNDING INFORMATION

Authors state no funding involved.

## AUTHOR CONTRIBUTIONS STATEMENT

This journal uses the Contributor Roles Taxonomy (CRediT) to recognize individual author contributions, reduce authorship disputes, and facilitate collaboration.

Name of Author	C	M	So	Va	Fo	I	R	D	O	E	Vi	Su	P	Fu
Satyanarayana Burada	✓	✓	✓	✓	✓	✓	✓	✓	✓	✓	✓		✓	
Kottala Padma	✓	✓				✓	✓	✓		✓	✓	✓	✓	✓

C : Conceptualization

M : Methodology

So : Software

Va : Validation

Fo : Formal analysis

I : Investigation

R : Resources

D : Data Curation

O : Writing - Original Draft

E : Writing - Review & Editing

Vi : Visualization

Su : Supervision

P : Project administration

Fu : Funding acquisition

## CONFLICT OF INTEREST STATEMENT

Authors state no conflict of interest.

## DATA AVAILABILITY

The authors confirm that the data supporting the findings of this study are available within the article.




## REFERENCES

- [1] B. Enayati, "Impact of IEEE 1547 standard on smart inverters and the applications in power systems," IEEE Power & Energy Society, 2020, doi: 10.17023/r323-bh61.
- [2] "IEEE standard for interconnection and interoperability of distributed energy resources with associated electric power systems interfaces--amendment 1: To provide more flexibility for adoption of abnormal operating performance category III," no. IEEE Standard 1547-2018 (Revision of IEEE Std 1547-2003). IEEE, Piscataway, NJ, USA, Mar. 09, 2020, doi: 10.1109/IEEESTD.2020.9069495.
- [3] A. Camacho, M. Castilla, J. Miret, L. G. de Vicuna, and R. Guzman, "Positive and negative sequence control strategies to maximize the voltage support in resistive-inductive grids during grid faults," *IEEE Transactions on Power Electronics*, vol. 33, no. 6, pp. 5362–5373, Jun. 2018, doi: 10.1109/TPEL.2017.2732452.
- [4] M. Mirhosseini, J. Pou, and V. G. Agelidis, "Single- and two-stage inverter-based grid-connected photovoltaic power plants with ride-through capability under grid faults," *IEEE Transactions on Sustainable Energy*, vol. 6, no. 3, pp. 1150–1159, Jul. 2015, doi: 10.1109/TSTE.2014.2347044.
- [5] G. Lammert, D. Premm, L. D. P. Ospina, J. C. Boemer, M. Braun, and T. Van Cutsem, "Control of photovoltaic systems for enhanced short-term voltage stability and recovery," *IEEE Transactions on Energy Conversion*, vol. 34, no. 1, pp. 243–254, Mar. 2019, doi: 10.1109/TEC.2018.2875303.
- [6] M. J. Morshed and A. Fekih, "A novel fault ride through scheme for hybrid wind/PV power generation systems," *IEEE Transactions on Sustainable Energy*, vol. 11, no. 4, pp. 2427–2436, Oct. 2020, doi: 10.1109/TSTE.2019.2958918.
- [7] P. Mishra, A. K. Pradhan, and P. Bajpai, "Voltage control of PV inverter connected to unbalanced distribution system," *IET Renewable Power Generation*, vol. 13, no. 9, pp. 1587–1594, Jul. 2019, doi: 10.1049/iet-rpg.2018.6219.
- [8] M. Islam, M. Nadarajah, and M. J. Hossain, "Short-term voltage stability enhancement in residential grid with high penetration of rooftop PV units," *IEEE Transactions on Sustainable Energy*, vol. 10, no. 4, pp. 2211–2222, 2019, doi: 10.1109/TSTE.2018.2883453.
- [9] H. Khan, S. J. Chacko, B. G. Fernandes, and A. Kulkarni, "Reliable and effective ride-through controller operation for smart PV systems connected to LV distribution grid under abnormal voltages," *IEEE Journal of Emerging and Selected Topics in Power Electronics*, vol. 8, no. 3, pp. 2371–2384, Sep. 2020, doi: 10.1109/JESTPE.2019.2918620.
- [10] M. Garnica, L. G. de Vicuna, J. Miret, M. Castilla, and R. Guzman, "Optimal voltage-support control for distributed generation inverters in RL grid-faulty networks," *IEEE Transactions on Industrial Electronics*, vol. 67, no. 10, pp. 8405–8415, Oct. 2020, doi: 10.1109/TIE.2019.2949544.
- [11] T. Roinila, T. Messo, and E. Santi, "MIMO-identification techniques for rapid impedance-based stability assessment of three-phase systems in DQ domain," *IEEE Transactions on Power Electronics*, vol. 33, no. 5, pp. 4015–4022, 2018, doi: 10.1109/TPEL.2017.2714581.
- [12] T. Roinila, M. Vilkkio, and J. Sun, "Broadband methods for online grid impedance measurement," in *2013 IEEE Energy Conversion Congress and Exposition*, IEEE, Sep. 2013, pp. 3003–3010, doi: 10.1109/ECCE.2013.6647093.
- [13] A. Sandali and A. Cheriti, "New adapted forms of PV optimal slope MPPT for a better grid connected PV system integration," in *2017 IEEE International Conference on Industrial Technology (ICIT)*, Toronto, ON, Canada: IEEE, 2017, pp. 446–451, doi: 10.1109/ICIT.2017.7913272.
- [14] J. Han, W. Jia, Y. Wang, L. Zhou, H. Hu, and Y. Ren, "An optimized strategy of switching crowbar improve LVRT of DFIG Based on RTDS," in *2020 IEEE Sustainable Power and Energy Conference (iSPEC)*, IEEE, Nov. 2020, pp. 775–780, doi: 10.1109/iSPEC50848.2020.9351162.




- [15] M. Y. Worku and M. A. Abido, "Grid-connected PV array with supercapacitor energy storage system for fault ride through," in *2015 IEEE International Conference on Industrial Technology (ICIT)*, IEEE, Mar. 2015, pp. 2901–2906, doi: 10.1109/ICIT.2015.7125526.
- [16] Y. Yang, P. Enjeti, F. Blaabjerg, and H. Wang, "Wide-scale adoption of photovoltaic energy: Grid code modifications are explored in the distribution grid," *IEEE Industry Applications Magazine*, vol. 21, no. 5, pp. 21–31, 2015, doi: 10.1109/MIAS.2014.2345837.
- [17] C. K. Das, O. Bass, G. Kothapalli, T. S. Mahmoud, and D. Habibi, "Overview of energy storage systems in distribution networks: Placement, sizing, operation, and power quality," *Renewable and Sustainable Energy Reviews*, vol. 91, pp. 1205–1230, Aug. 2018, doi: 10.1016/j.rser.2018.03.068.
- [18] A. K. Abdelsalam, A. M. Massoud, S. Ahmed, and P. N. Enjeti, "High-performance adaptive perturb and observe MPPT technique for photovoltaic-based microgrids," *IEEE Transactions on Power Electronics*, vol. 26, no. 4, pp. 1010–1021, Apr. 2011, doi: 10.1109/TPEL.2011.2106221.
- [19] A. Pandey, N. Dasgupta, and A. K. Mukerjee, "High-performance algorithms for drift avoidance and fast tracking in solar MPPT system," *IEEE Transactions on Energy Conversion*, vol. 23, no. 2, pp. 681–689, Jun. 2008, doi: 10.1109/TEC.2007.914201.
- [20] B. R. Naidu, S. Jose, D. Singh, and P. Bajpai, "A unified distributed control strategy for DC microgrid with hybrid energy storage devices," in *2018 20th National Power Systems Conference (NPSC)*, IEEE, Dec. 2018, pp. 1–6, doi: 10.1109/NPSC.2018.8771836.
- [21] B. R. Naidu and P. Bajpai, "Voltage fault ride-through operation of solar PV generation," in *Fundamentals and Innovations in Solar Energy*, S. N. Singh, P. Tiwari, and S. Tiwari, Eds., Singapore: Springer, 2021, pp. 467–497, doi: 10.1007/978-981-33-6456-1\_19.
- [22] M. Karimi-Ghartema, *Enhanced phase-locked loop structures for power and energy applications*, vol. 9781118795. Piscataway, NJ, USA: Wiley-IEEE Press, 2014. doi: 10.1002/9781118795187.
- [23] L. Steinhäuser, M. Coumont, S. Weck, and J. Hanson, "Comparison of RMS and EMT models of converter-interfaced distributed generation units regarding analysis of short-term voltage stability," in *NEIS 2019 - Conference on Sustainable Energy Supply and Energy Storage Systems*, 2019, pp. 31–36.
- [24] B. R. Naidu, P. Bajpai, and C. Chakraborty, "Energy storage unit for dynamic voltage support in distribution networks," in *ICPS 2021 - 9th IEEE International Conference on Power Systems: Developments towards Inclusive Growth for Sustainable and Resilient Grid*, 2021, pp. 1–6, doi: 10.1109/ICPS52420.2021.9670110.
- [25] M. Y. Worku and M. A. Abido, "Grid-connected PV array with supercapacitor energy storage system for fault ride through," in *2015 IEEE International Conference on Industrial Technology (ICIT)*, 2015, pp. 2901–2906, doi: 10.1109/ICIT.2015.7125526.

## BIOGRAPHIES OF AUTHORS



**Satyanarayana Burada**    received B.Tech. degree in Electrical and Electronics Engineering from JNTU Kakinada, India, in 2012, M.Tech. degree in Power Systems from National Institute of Technology (NIT), Surat, India in 2016, and currently pursuing Ph.D. in the grid-connected photovoltaic systems area from Andhra University, Visakhapatnam, India. Recently, he published one Scopus-indexed journal article in 2023 and presented papers in 2 IEEE conferences held at Delhi Technological University in 2016 and Amity University in 2017. From 2016 until now, he has been a lecturer in the Department of Electrical and Electronics Engineering, Anil Neerukonda Institute of Technology and Sciences, Visakhapatnam, India. He can be contacted at email: satyanarayana.eee@anits.edu.in.



**Kottala Padma**    has done her B.Tech. from Sri Venkateswara University in 2005, M.Tech. in Power Systems from Andhra University in 2010, and Ph.D. from Andhra University in 2015. Presently working as an Associate Professor of the Electrical Engineering Department at Andhra University, Visakhapatnam, India. She has published 14 papers in SCI, Scopus, Web of Science-indexed journals, and 2 papers in Springer book chapters. Her research interests include power system aspects, renewable energy systems, microgrids, internet of things, soft computing techniques, transmission, and distribution systems. She has guided 2 Ph.D. She has guided 2 Ph.D. students and is currently guiding 8 research scholars. She has also successfully supervised 30 postgraduate (PG) theses. She has been presented with the Global Teacher Award and the Best Research Award. She can be contacted at email: dr.kpadma@andhrauniversity.edu.in.